frontiers | Frontiers in Materials

TYPE Original Research
PUBLISHED 02 June 2025
DOI 10.3389/fmats.2025.1619529

OPEN ACCESS

EDITED BY
Jiuwen Bao,
Qingdao University of Technology, China

REVIEWED BY
Amir Ali Shahmansouri,
Washington State University, United States
Qiang Wang,
Hebei University of Science and Technology, China

*CORRESPONDENCE
Xin Wang,
20232210079@stu.kust.edu.cn

RECEIVED 28 April 2025
ACCEPTED 23 May 2025
PUBLISHED 02 June 2025

CITATION
Liu J, Huang P, Gan H, Wang X and Liu Z (2025) Novel mechanism of sulfate erosion mitigation in cement mortar using CF-based densifier: microstructural and durability perspectives.
Front. Mater. 12:1619529.
doi: 10.3389/fmats.2025.1619529

Novel mechanism of sulfate erosion mitigation in cement mortar using CF-based densifier: microstructural and durability perspectives

Jianye Liu[1], Peishan Huang[1], Hehao Gan[1], Xin Wang[2]* and Zhuo Liu[2]

[1]Shanghai Transportation Construction General Contracting Co., Ltd, Shanghai, China, [2]Faculty of Civil Engineering and Mechanics, Kunming University of Science and Technology, Kunming, China

Cementitious materials are widely used in marine and alkaline environments, where sulfate erosion resistance significantly influences structural durability and safety. To address this challenge, this study systematically evaluated the effectiveness of CF-S2 densifier in enhancing sulfate erosion resistance of cement mortar. The performance of CF-based densifier mortars with varying dosages was assessed by compressive strength, mercury intrusion porosimetry (MIP), SO_4^{2-} concentration distribution, and dry-wet cyclic sulfate erosion tests. The results indicated that the CF-based densifier optimized the pore size distribution by reducing the proportion of harmful pores (≥100 nm), especially macropores (>1,000 nm). Meanwhile, it increased the proportion of transition pores (10–100 nm) and improved pore tortuosity, effectively hindering aggressive ion penetration. After 60 wet-dry cycles, compared to ordinary Portland cement (OPC) mortar, the compressive strength and corrosion resistance coefficient of mortar containing 0.1% CF-S2 increased by 36.4% and 41.5%, respectively, along with significantly reduced surface erosion damage. Moreover, SO_4^{2-} concentration distribution tests showed consistently lower SO_4^{2-} concentrations at all measured depths in densifier mortar, confirming improved sulfate resistance. This study demonstrates that CF-based densifier significantly enhances the mechanical properties and sulfate erosion resistance of cement mortar, providing an effective strategy for improving durability of cement-based materials and offering broad prospects for engineering applications.

KEYWORDS

cementitious materials, sulfate attack, dry-wet cycles, sulfate ion distribution, pore structure

1 Introduction

Concrete has become the most widely utilized construction material globally, owing to its abundant raw materials, mature preparation technologies, and versatile engineering applicability (Tan et al., 2022; Zheng et al., 2023; Zhao et al., 2024). However, ordinary concrete exhibits poor resistance to sulfate attack in aggressive

environments such as oceans and saline soils, resulting in structural degradation and considerable durability loss (Neville, 2004; Pang et al., 2024). Given the widespread presence of sulfate-rich environments worldwide, sulfate attack significantly increases maintenance expenditures and severely compromises structural safety and reliability. Such deterioration often results in the premature failure of concrete structures, causing substantial economic losses (Ikumi et al., 2016; Sun et al., 2018). Therefore, developing effective strategies to improve the sulfate erosion resistance of cementitious materials has become imperative in extending the service life of concrete structures.

In recent years, extensive research has been conducted to elucidate sulfate attack mechanisms and develop protective strategies for concrete structures. According to Motohiro Ohno and Thidar Aye et al. (Aye and Oguchi, 2011; Ohno and Maekawa, 2025), sulfate attack on concrete can be classified into two primary types: ISA (Internal Sulfate Attack) occurs when SO_4^{2-} originates from within the concrete mixture, whereas ESA (External Sulfate Attack) involves the penetration of external SO_4^{2-} into the concrete matrix (Liu et al., 2024; Yu and Zhang, 2018). SO_4^{2-} reacts with hydration products, particularly calcium aluminate hydrates and calcium hydroxide, forming expansive compounds such as ettringite and gypsum. This leads to expansion, cracking, and further deterioration of cementitious materials (Sun et al., 2013; Bary et al., 2014; Qin et al., 2020). Moreover, the deterioration of cementitious materials is significantly accelerated under dry-wet cyclic conditions, leading to intensified damage. In addition to chemical degradation, sulfate crystallization-induced physical damage further compromises the structural integrity of mortar (Wang et al., 2020). Studies have demonstrated that the accumulation of sulfate crystals within fine pores generates crystallization pressure, causing cracking and surface spalling of cementitious materials. This further facilitates the penetration of aggressive ions into the mortar, accelerating its deterioration (Wang et al., 2025; Aye and Oguchi, 2011). Cementitious materials with high porosity and low pore tortuosity exhibit increased microstructural connectivity, allowing external SO_4^{2-} to readily penetrate the matrix and accelerate deterioration (Wei et al., 2021). Thus, sulfate attack not only severely deteriorates cementitious materials but also involves highly complex mechanisms. The rate and extent of deterioration in sulfate-rich environments depend on numerous factors, including sulfate concentration, exposure duration, water-cement ratio, material composition, and cement matrix pore structure (Akpinar and Casanova, 2010; Zhang et al., 2017; Singh et al., 2024).

To enhance the durability of concrete structures in sulfate-rich environments, traditional protective strategies primarily include: (1) reducing the water-to-cement ratio (W/C) to improve the compactness of cementitious materials, thereby minimizing the infiltration of aggressive solutions (Irassar, 2009; Bassuoni and Rahman, 2016); (2) incorporating mineral admixtures (e.g., fly ash, blast furnace slag, and silica fume) to refine the microstructure and reduce porosity of cementitious materials (Kou and Poon, 2013; Quan et al., 2021); (3) limiting the C_3A content in cement clinker to suppress ettringite formation (Nosouhian et al., 2019; Andrade Neto et al., 2021); and (4) selecting aggregates with appropriate type, particle size distribution, and quality to mitigate sulfate-induced deterioration (Qi et al., 2017; Campos et al., 2018; Cheng et al., 2022). Although traditional methods can enhance sulfate resistance to a certain degree, they are often cumbersome, expensive, and inadequate for fully preventing sulfate attack. Particularly in environments subject to frequent dry-wet cycles, maintaining the durability of cementitious materials remains challenging.

This study systematically investigated the effects of different dosages of a commercial CF-S2 densifier on the mechanical properties, pore structure, and sulfate erosion resistance of cement mortars. Mercury intrusion porosimetry (MIP) was employed to characterize the pore structure of CF-based densifier mortars, clarifying its role in pore structure refinement and elucidating the underlying mechanism of enhanced sulfate resistance. The sulfate erosion resistance of CF-S2 densifier mortar under sulfate dry-wet cycling conditions was comprehensively evaluated by analyzing its apparent morphology, compressive strength, corrosion resistance coefficient, SO_4^{2-} concentration distribution, and microscopic features. This study provides both theoretical insights and experimental evidence for the application of CF-S2 densifier as an effective modification strategy to significantly enhance the durability of cementitious materials. The findings offer substantial academic contributions and promising engineering applications.

2 Materials and experimental methods

2.1 Materials

The cement mortar mixtures used in this study consisted of ordinary Portland cement, ISO standard sand, a polycarboxylate-based water-reducing agent, CF-based densifier, and tap water. The cement used was ordinary Portland cement (P·O 42.5 grade) supplied by Yunnan Huaxin Cement Co., Ltd. (Kunming, China). Its chemical composition is presented in Table 1. The ISO standard sand was provided by Xiamen ISO Standard Sand Co., Ltd. (Xiamen, China). A polycarboxylate-based high-performance water-reducing agent was provided by Shanxi Feike New Material Technology Co., Ltd. The CF-based densifier was supplied by Landun (Yunnan) Engineering Technology Co., Ltd. The CF-based densifier is a commercial, proprietary calcium fluoro-silicate nanodensifier, primarily composed of 15–20 nm amorphous SiO_2, a small amount of Ca-based stabilizer, trace F^- (<0.1 wt%), and ≤0.5 wt% of 3-propylsulfonic acid silane. Laboratory tap water was used for mixing purposes.

2.2 Sample preparation

In this study, four types of cement mortar specimens were prepared with a water-to-cement ratio (W/C) of 0.4. The mixing proportions are listed in Table 2, where OPC represents the reference mortar without densifier, S2-0.1 indicates mortar containing 0.1 wt% CF-based densifier relative to the mass of cement, and the remaining mixtures are named similarly. First, the densifier was dispersed in water along with the water-reducing agent, and the mixture was stirred using a magnetic stirrer for 2 min. Subsequently, the prepared solution was transferred into a cement-sand mixer and blended with cement for 1 min. Then, standard sand was gradually and uniformly incorporated into the cement slurry. The fresh mortar mixture was prepared by sequential mixing at low-speed for 1 min,

TABLE 1 Chemical compositions of cement (mass%).

Materials	CaO	SiO_2	Fe_2O_3	Al_2O_3	K_2O	TiO_2	Na_2O	SO_3	MgO
Cement	62.2053	19.4219	3.513	6.2036	0.7808	1.2325	0.3484	3.9288	1.9501

TABLE 2 Mixture proportions of modified mortar (g).

Specimen ID	Cement	Standard sand	Water	Water reducer	CF-S2
OPC	506	1,440	202.4	1.116	0
S2-0.1	506	1,440	202.4	0.947	0.506 (0.1%)
S2-0.15	506	1,440	202.4	0.947	0.759 (0.15%)
S2-0.2	506	1,440	202.4	0.947	1.012 (0.2%)

high-speed for 30 s, and again low-speed for 30 s. Finally, the fresh mortar was cast into 40 mm × 40 mm × 160 mm molds and compacted using a vibrating table. After casting, specimens were demolded and cured according to GB/T 50081-2019 (Chinese Standard for Test Methods of Physical and Mechanical Properties of Concrete) (GB/T 50081-2019, Standard for test methods of concrete physical and mechanical properties, 2019).

2.3 Test methods

2.3.1 Mechanical properties test

The compressive strength of the cement mortar specimens was tested at curing ages of 3, 7, and 28 days using a universal testing machine, in accordance with GB/T 17671-2021 ("Test Method for Strength of Cementitious Sand (ISO Method)") (GB/T 17671-2021,Test method of cement mortar strength (ISO method), 2021). A force-controlled loading rate of 2400 N/s was applied during the tests. The compressive strength of each group was calculated as the arithmetic mean value of six specimens.

2.3.2 MIP test

Mercury intrusion porosimetry (MIP) was used to analyze the porosity and pore size distribution of cement mortar specimens at a curing age of 28 days. According to the classification proposed by [Author Name et al.], the pores in mortar can be divided into four categories based on size: gel pores (<10 nm), transition pores (10–100 nm), capillary pores (100–1,000 nm), and macropores (>1,000 nm) (Guo et al., 2021). The Corrugated Pore Structure Model (CPSM) was employed to characterize the curvature of the pore structure (Salmas and Androutsopoulos, 2001). Based on the CPSM, the curvature of mortar can be quantitatively determined using Equation 1:

$$\tau = 4.6242 \ln\left(\frac{4.996}{1-\alpha_{en}} - 1\right) - 5.8032 \quad (1)$$

where τ and α_{en} represent tortuosity and pore closure fraction, respectively. The pore closure fraction α_{en} is defined as the ratio of the pore closure volume to the total intrusion volume (Mohan et al., 2023).

2.3.3 Dry-wet cycling sulfate attack

Sulfate erosion tests under dry-wet cyclic conditions were performed according to GB/T 50082-2009 (Standard for Test Methods of Long-term Properties and Durability of Ordinary Concrete) (GB/T 50082-2009,Standard for test methods of long-term performance and durability of ordinary concrete, 2009) to investigate the effects of dry-wet cycles on the surface morphology, mass loss rate, and compressive strength of CF-S2 densifier mortars. After standard curing for 26 days, the specimens were dried in an oven at 65°C ± 5°C for 48 h. Each sulfate dry-wet cycle consisted of four sequential stages: immersion (soaking), air drying, oven drying, and cooling.

As illustrated in Figure 1, the specimens were first immersed in a 5 wt% Na_2SO_4 solution for 15 h, followed by air drying for 1 h. Subsequently, the specimens were oven-dried at 65°C ± 5°C for 6 h and then ventilated and cooled for 2 h. Each dry-wet cycle lasted 24 h, and a total of 60 cycles were conducted. The sulfate solution was renewed at the end of each cycle to maintain stable pH and sulfate ion concentration during the erosion process. Control specimens, not exposed to sulfate attack, were maintained under standard curing conditions for the same duration. Finally, the compressive strengths of specimens (standard-cured and sulfate-eroded) were tested after 15, 30, and 60 dry-wet cycles, respectively.

2.3.3.1 Compressive strength and corrosion resistance coefficient after erosion

In this study, the compressive strength test of sulfate dry-wet cycle and standard curing control mortar specimens was carried out according to GB/T 17671-2021 "Test Method for Strength of Cement Cementitious Sand (ISO Method)" (GB/T 17671-2021,Test method of cement mortar strength (ISO method), 2021)using a universal testing machine. The sulfate corrosion resistance of the mortar was evaluated by the compressive strength corrosion resistance coefficient K_f, which was calculated using Equation 2:

$$K_f = \frac{f_d}{f_c} \times 100\% \quad (2)$$

Where K_f is the compressive strength corrosion resistance coefficient of mortar specimens, f_d represents the compressive

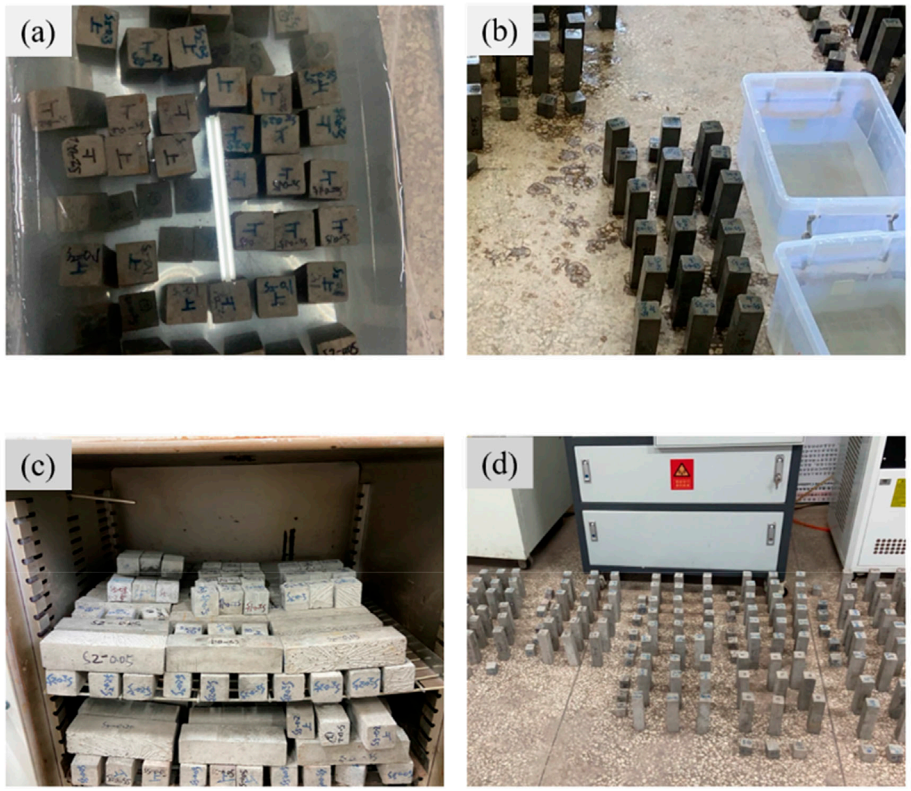

FIGURE 1
Procedure of dry and wet cycle. **(a)** Soaking Phase. **(b)** Air Drying Phase. **(c)** Oven Drying Phase. **(d)** Cooling Phase.

strength of specimens after different wet-dry cycle times, f_c is the compressive strength of specimens of the same age maintained in the standard curing room, and d represents the number of wet-dry cycles.

2.3.3.2 SO_4^{2-} concentration test

To ensure unidirectional sulfate ion penetration, the side and bottom surfaces of mortar specimens were uniformly sealed with epoxy resin. After 60 dry-wet cycles, mortar specimens were sliced at 2 mm intervals from the unsealed top surface downward to a depth of 18 mm using a cutting machine. The mortar slices were crushed using a ceramic mortar and ground into powder samples, which passed through a 0.075 mm (No. 200) sieve. The SO_4^{2-} content in powder samples was determined by the barium sulfate gravimetric method, according to GB/T 176-2008; GB/T 176-2008,Methods for chemical analysis of cement, 2008). The measurement procedure for SO_4^{2-} concentration is illustrated in Figure 2. The sulfate concentration at different depths (expressed as mass percentage of SO_3, accurate to 0.01%) was calculated using Equation 3.

$$\Delta W_{SO_3} = \frac{0.343 \times (m_2 - m_{1)}}{m_0} \times 100\% \quad (3)$$

ΔW_{SO_3} represents the amount of sulfate in the powder (related to SO_3), m_0 is the initial weight of the powder (g), m_1 is the weight of the crucible (g), m_2 is the combined weight of the precipitate and the crucible (g), and 0.343 is the conversion factor between $BaSO_4$ and SO_3 based on their relative molecular masses.

3 Results and discussion

3.1 Conventional mechanical properties

Figure 3 shows the compressive strength of mortar specimens with different dosages of densifier at ages of 3, 7, and 28 days. It can be seen that with the increase in the dosage of the CF-based densifier, the compressive strength at 7 days generally exhibits an increasing trend. The compressive strengths at 3 and 28 days initially increase and subsequently exhibit a slight decrease with increasing densifier dosage. Overall, mortar specimens containing 0.1% CF-based densifier exhibit the highest compressive strength at both early (3 and 7 days) and later stages (28 days). The results demonstrate that the CF-based densifier significantly contributes to the enhancement of compressive strength in cement mortar.

3.2 Pore structure analysis

Studies have shown that increasing the degree of matrix densification and reducing permeability are key to enhancing the sulfate erosion resistance of cementitious materials (Zhang et al., 2020). Povindar Kumar Mehta et al. (Povindar Kumar Mehta and Monteiro, 1986)concluded that microscopic pores with diameters greater than 100 nm are classified as harmful pores, and an increase in their number significantly deteriorates the mechanical properties of cementitious materials. Chen et al. (Chen et al., 2023) stated that

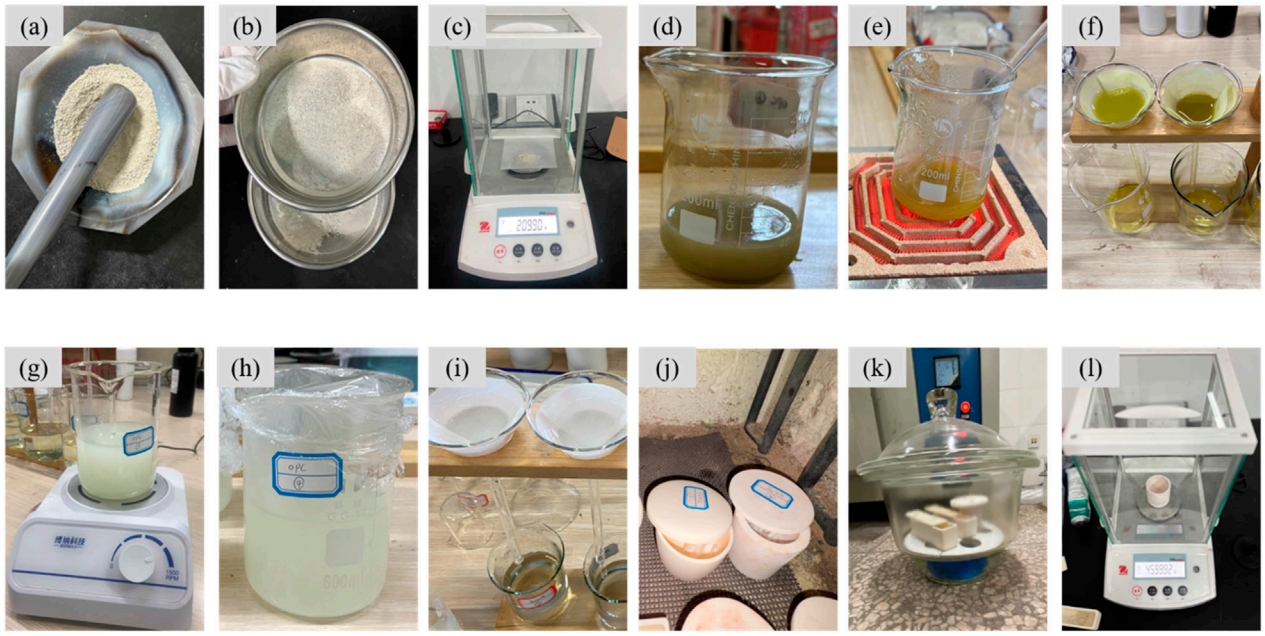

FIGURE 2
Analytical procedure for determining SO_4^{2-} concentration. **(a)** Grinding. **(b)** Sieve. **(c)** Weighing. **(d)** Dissolution. **(e)** Heating. **(f)** Qualitative Filtration. **(g)** Add BaCl2. **(h)** Resting. **(i)** Quantitative filtration. **(j)** Ignition. **(k)** Cooling. **(l)** Weighing.

pores larger than 1,000 nm are critical to concrete permeability, and the higher their proportion, the greater the material's permeability. Therefore, the durability of concrete can be effectively improved by reducing the proportion of large pores (>1,000 nm) and increasing the proportion of transition pores (10–100 nm) (Zhang et al., 2024).

To investigate the influence of the CF-based densifier on the microscopic pore structure, mortars with different densifier dosages were characterized using mercury intrusion porosimetry (MIP). Figure 4 presents the pore size distribution curves and percentages for OPC, S2-0.1, and S2-0.2 mortars at 28 days. As shown in Figures 4a,b, the percentage of gel pores (<10 nm) in S2-0.1 and S2-0.2 mortars is lower than in OPC, indicating that the densifier has a limited influence on refining gel pores. Figures 4a,b also demonstrate that the proportions of capillary pores (100–1,000 nm) and macropores (>1,000 nm) in the cement mortars significantly decreased with the addition of the densifier, particularly macropores. Compared to OPC, the proportions of macropores in S2-0.1 and S2-0.2 mortars decreased by 18.95% and 32.5%, respectively, while the proportions of transition pores (10–100 nm) increased by 11% and 13.7%, respectively. Pore structure characteristics are crucial factors influencing cementitious materials' durability, which largely depends on pore structure and permeability (Li et al., 2018). The transport of aggressive ions in porous materials, such as cement mortar, depends on pore tortuosity, and mortar permeability decreases as tortuosity increases (Dhandapani and Santhanam, 2020). Therefore, mortar with higher tortuosity generally exhibits better sulfate attack resistance (Kumar and Bhattacharjee, 2003; Xiangpeng et al., 2023). The porosities of OPC, S2-0.1, and S2-0.2 mortars were 10.06%, 9.78%, and 10.56%, respectively, while their pore curvatures were 3.64, 3.72, and 3.92, respectively. The pore curvature of S2-0.2 mortar increased by 7.69% compared to OPC mortar. This increase indicates that the CF-S2 densifier refines mortar pore structure, enhancing its durability.

These results indicate that the densifier increased the proportion of transition pores (10–100 nm), reduced the proportion of harmful pores (>100 nm), and significantly enhanced pore tortuosity, thereby improving the sulfate erosion resistance of cement mortar. The increase in pore curvature enhances the complexity of pore pathways, leading to slower water vapor diffusion and longer transport distances, which in turn mitigates internal drying rates and suppresses the accumulation of shrinkage strain.

3.3 Resistance to dry and wet cyclic sulfate attack

3.3.1 Surface morphology

Figure 5 shows the surface morphology of mortar specimens after 60 days of dry-wet cyclic sulfate attack. As shown in Figure 5, the OPC samples exhibited obvious surface cracks and severe cracking at the corners and edges. In contrast, no visible cracks appeared on the surfaces of S2-0.1, S2-0.15, and S2-0.2 specimens. To accurately quantify the degree of damage to the cement mortar, the surface deterioration grade was evaluated according to the criteria reported in previous studies (Fang et al., 2022; Fang et al., 2023), as listed in Table 3. A higher deterioration grade indicates more severe mortar damage. The results indicate that the OPC mortar exhibited the highest deterioration grade (grade 4). In contrast, the deterioration grades of S2-0.15 and S2-0.2 mortars were grade 1, and the S2-0.1 mortar showed no deterioration (grade 0). These findings demonstrate that mortars modified with CF-S2

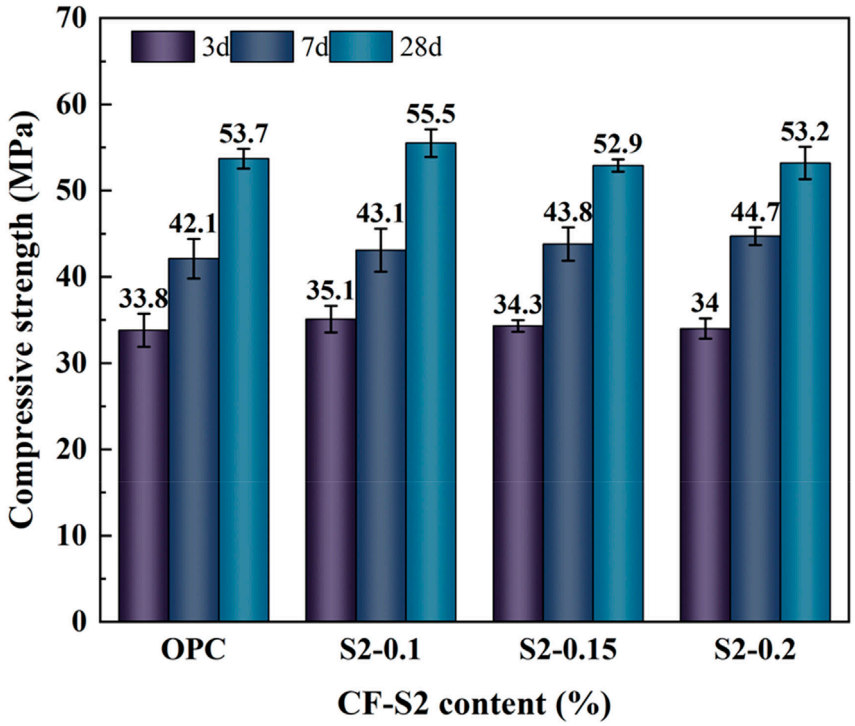

FIGURE 3
Conventional mechanical properties.

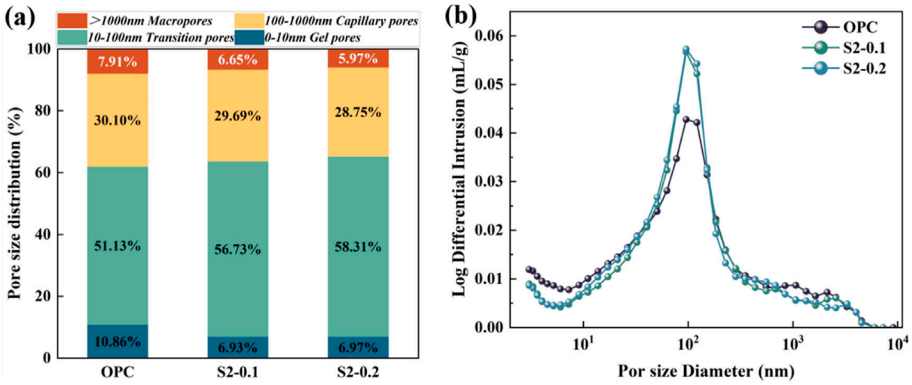

FIGURE 4
Pore-size distribution of mortars after 28 days water curing: **(a)** Pore-size distribution percentage of mortar; **(b)** Pore-size distribution curve of mortar.

densifier maintained superior surface integrity after 60 days of dry-wet cyclic sulfate attack, indicating that CF-S2 addition effectively mitigated surface deterioration.

3.3.2 Distribution of SO_4^{2-} concentration

Figure 6 illustrates the SO_4^{2-} concentration profile of each mortar after 60 wet–dry sulfate cycles. The concentration decreased progressively with depth, because the surface layer was directly exposed to the aggressive environment whereas the interior experienced limited ion ingress. At every depth, the OPC specimens exhibited higher SO_4^{2-} concentrations than the CF-S2-modified mortars, with the difference most pronounced at 2 mm and 6 mm. Specifically, the OPC values were higher by 93.7%, 112.5%, 29.4%, 31.3% and 42.9% than those of S2-0.15 at depths of 2 mm, 6 mm, 10 mm, 14 mm and 16 mm, respectively. These findings are consistent with the greater compressive-strength reductions and severe surface cracking observed in OPC after the wet–dry cycles. In contrast, the CF-S2 mortars maintained lower SO_4^{2-} concentrations at all depths and showed no visible cracking or strength deterioration, confirming that CF-S2 effectively limits sulfate penetration throughout the matrix.

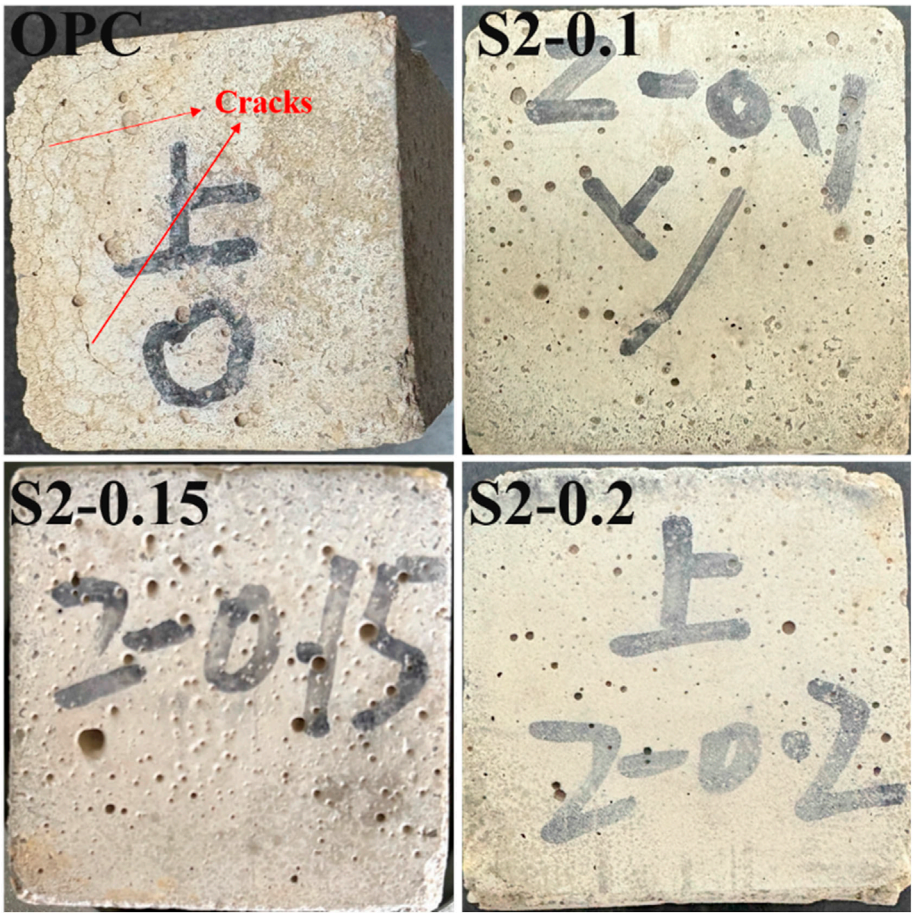

FIGURE 5
Apparent morphology of cement mortar after 60 cycles of dry and wet sulfate erosion.

TABLE 3 Evaluation criteria for surface deterioration grade (adapted from [46,47]).

Grade	Deterioration characteristics	Grade	Deterioration characteristics
0	No observable surface damage	5	Widespread cracking and volumetric expansion
1	Minor degradation at corners and edges	6	Progressive expansion with sidewall damage
2	Degradation extends to corners, edges, and base	7	Advanced expansion and surface spalling
3	Visible cracks at corners and edges	8	Severe degradation across entire specimen
4	Severe edge cracking and material expansion	9	Structural collapse

3.3.3 Compressive strength and corrosion resistance factor

Figure 7a shows the compressive strength evolution of ordinary Portland cement (OPC) mortar specimens and CF-S2 densifier-modified mortar specimens subjected to 15, 30, and 60 dry-wet sulfate cycles. The compressive strength of the OPC samples initially increased during the early stages of dry-wet cycling, reaching a peak value of 64.2 MPa at 15 days, and then gradually decreased with prolonged erosion. In contrast, the compressive strength of the densifier mortar specimens continued to increase throughout the erosion period. Notably, after 60 dry-wet cycles, the compressive strength of the OPC specimen decreased to 54.7 MPa, while that of the S2-0.1 mortar increased to 74.6 MPa, representing a notable enhancement of 36.4% compared with the OPC mortar. Furthermore, compressive strengths of other CF-S2-modified mortar specimens were also consistently higher (generally exceeding 30.5%) compared to OPC mortars, demonstrating that the CF-S2 densifier significantly improved the sulfate erosion resistance of mortar.

During sulfate erosion, SO_4^{2-} ions penetrate the mortar matrix under dry-wet cycles, generating expansive erosion products (such as calcium alumina and gypsum) and sulfate crystals. These

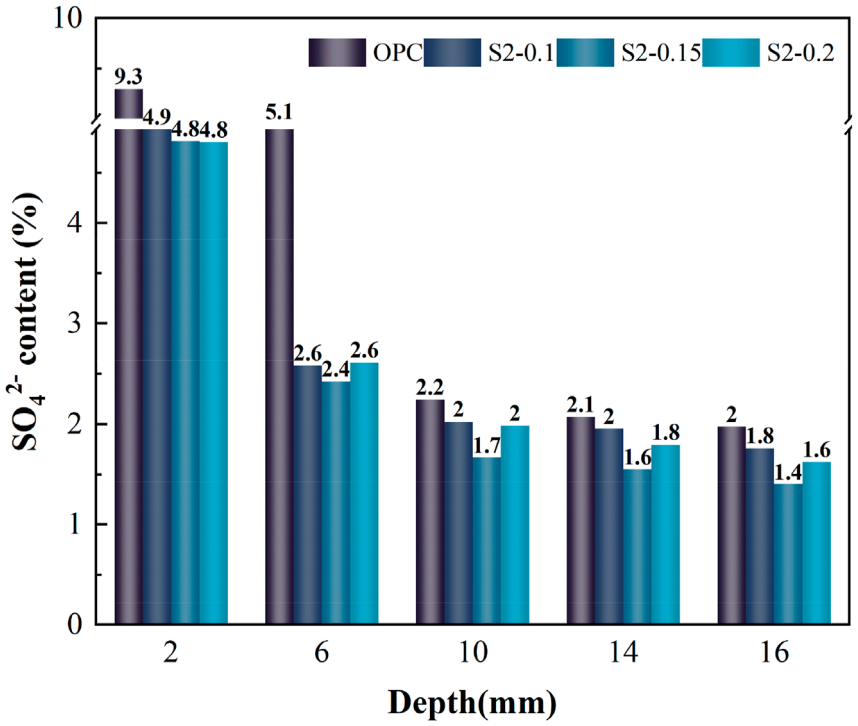

FIGURE 6
SO_4^{2-} concentration distribution at different depths of cement mortar after 60 days of dry-wet cyclic sulfate erosion.

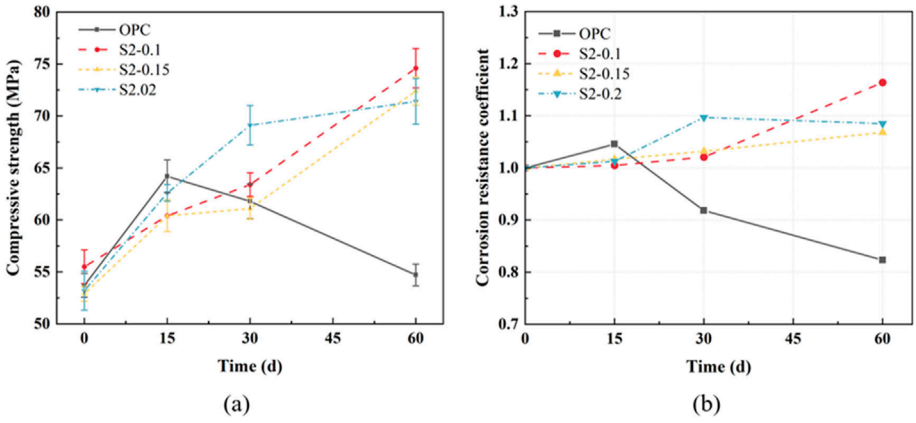

FIGURE 7
Evolution of mortar performance during sulfate attack (0-60 days): **(a)** compressive strength; **(b)** corrosion-resistance coefficient.

expansive products initially fill the pores and microcracks within the mortar, leading to matrix densification and a temporary increase in compressive strength at early stages. However, with prolonged erosion, the continuous formation of expansive products eventually exceeds the load-bearing capacity of the mortar matrix, causing microstructural deterioration, cracking, and expansion. This ultimately reduces the compressive strength, macroscopically manifesting as surface cracking or spalling, consistent with the observations in Figure 5.

Figure 7b shows the evolution of corrosion resistance coefficients of ordinary Portland cement (OPC) mortar specimens and CF-based densifier mortar specimens after 15, 30, and 60 days of dry-wet cyclic sulfate erosion. Similar to compressive strength trends, the corrosion resistance coefficient of OPC specimens initially increased in early erosion stages and subsequently decreased with prolonged erosion. In contrast, the corrosion resistance coefficient of CF-based densifier mortar specimens steadily increased throughout the erosion period. After 60 days of erosion,

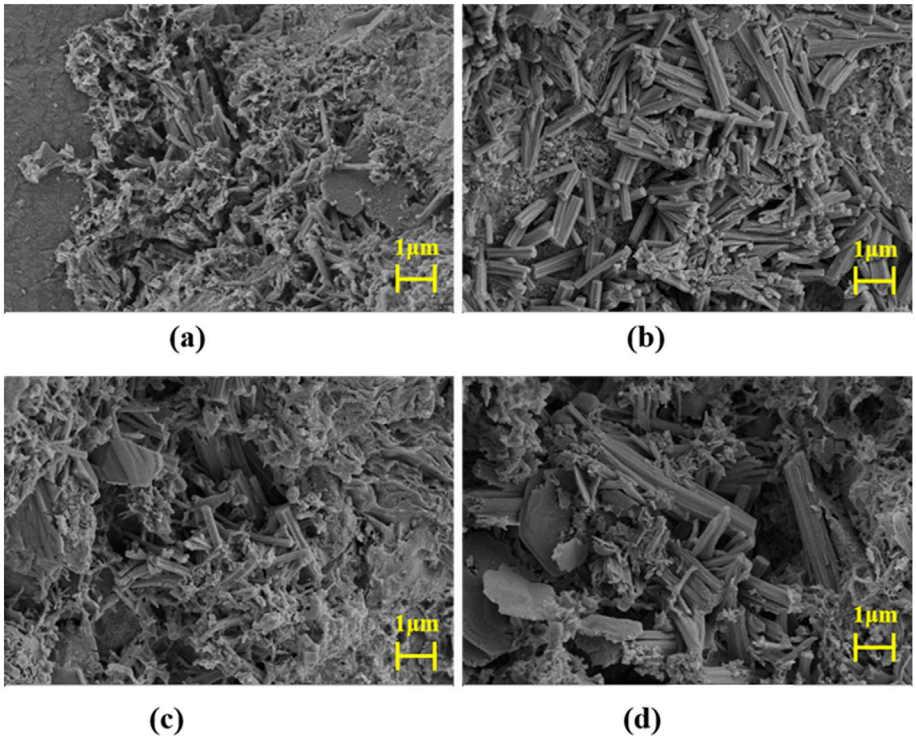

FIGURE 8
SEM images showing the microscopic morphology of mortar subjected to 60 days of dry-wet cycling in sulfate solution. **(a)** OPC. **(b)** S2-0.1. **(c)** S2-0.15. **(d)** S2-0.2

the corrosion resistance coefficient of the S2-0.1 specimen increased by 41.5% compared to the OPC specimen, while corrosion resistance coefficients of other CF-S2-modified specimens were consistently higher (generally exceeding 30.5%) compared to the OPC specimen. The results presented in Figures 7a,b demonstrate that the CF-S2 densifier significantly enhances the sulfate erosion resistance of cement mortar under dry-wet cyclic conditions.

3.3.4 SEM analysis

The microscopic morphology of each mortar sample after 60 days of dry-wet cycling in sulfate solution was observed using SEM, as shown in Figure 8. After 60 days of dry-wet cycling, significant cracking and crack propagation were observed in the OPC samples, accompanied by abundant short-columnar and needle-like crystals, along with loose, flocculent C-S-H gel distributed around the cracks. These short-columnar and needle-like crystals were identified as erosion products, predominantly calcite crystals (He and Lu, 2023; 2024; He et al., 2023). The internal stresses induced by the expansion of these erosive products exceeded the tensile strength capacity of the mortar matrix, causing cracking and deterioration of compressive strength in the OPC samples. In contrast, the S2-0.1 and S2-0.15 mortar samples exhibited a significantly denser microstructure, attributed primarily to the effective filling of pores by calcite crystals formed during sulfate erosion. The interlocking morphology of these calcite crystals further contributed to the enhancement of mortar strength. The microstructural observations are consistent with the trends observed in surface deterioration, compressive strength evolution, and corrosion resistance coefficients discussed previously.

3.4 Sustainability, cost and field implementation

As CF-S2 is a commercial product intended for engineering-scale use, its environmental compatibility, cost-effectiveness, and field feasibility are important considerations for practical application. This section briefly discusses these aspects based on the material's composition, lifecycle impact, and on-site implementation parameters.

The CF-S2 densifier presents a favourable sustainability profile. It is a water-based product with VOC <10 g L^{-1} and an active-solids content of ≈28 wt%, composed mainly of amorphous SiO_2 and Ca-bearing species with only trace F^- (<0.1 wt%). In service, the fluoride rapidly precipitates as CaF_2 within the pore network, giving a calculated long-term leachate level below 0.05 mg L^{-1}, well under the Class III surface-water limit of GB/T 14848-2022. Consequently, CF-S2 can be classified as a low-toxicity, low-emission densifier whose environmental burden is comparable to that of conventional colloidal-silica treatments.

From an economic standpoint, the recommended dosage of 0.10 wt% raises the fresh-material cost of ordinary Portland cement (OPC) mortar by only ≈1.6%. A simple life-cycle assessment shows that extending the design service life from 20 to 30 years translates

into a 15%–25% reduction in combined maintenance and end-of-life costs. Implementation is straightforward: CF-S2 is diluted with tap water and introduced during normal mixing, requiring no additional equipment or labour beyond standard batching and placement procedures.

Field application nevertheless demands dosage optimisation. Exceeding 0.10 wt% has shown no statistically significant durability benefit in this study while unnecessarily increasing material cost. Practitioners are therefore advised to tailor the dose to the expected sulfate exposure class and concrete permeability, to balance performance gains against economic outlay.

4 Conclusion

The aim of this study was to elucidate the mechanism by which CF densifier influences the properties of cement mortar. The effects of CF-S2 densifier on the mechanical properties, pore structure, and sulfate erosion resistance of cement mortar were systematically investigated through compressive strength tests, pore structure analysis by mercury intrusion porosimetry (MIP), and sulfate erosion experiments under dry-wet cycles. The main conclusions are as follows:

(1) The MIP results indicate that the CF-S2 densifier significantly improves the pore structure of cement mortar. The proportion of harmful pores (≥100 nm) was notably reduced, particularly for macropores (>1,000 nm), while the proportion of transition pores (10–100 nm) increased. Furthermore, the addition of CF-S2 densifier enhanced the tortuosity of the mortar and reduced its permeability.

(2) By comparing the SO_4^{2-} concentrations in OPC and CF-S2 densifier mortar at different depths, it was found that the SO_4^{2-} content in CF densifier mortar was consistently lower than in OPC. This distinct concentration gradient confirms that the CF-S2 densifier effectively inhibits the penetration of sulfate ions, thereby reducing structural damage from sulfate attack.

(3) The results of the dry-wet cyclic sulfate erosion test revealed that after 60 cycles, the compressive strength of OPC samples decreased from 64.2 MPa to 54.7 MPa, accompanied by visible surface cracks and severe deterioration (grade 4). In contrast, the mortar containing 0.1% CF-S2 densifier achieved a compressive strength of 74.6 MPa (36.4% higher than OPC) and exhibited a corrosion resistance coefficient that was 41.5% higher, with no visible surface deterioration. These results confirm the significant role of CF densifier in mitigating sulfate erosion and enhancing mortar resistance, with an optimal dosage of 0.1% by mass of cementitious materials.

(4) This study provides a theoretical and experimental basis for the application of CF-S2 densifier in cementitious materials, offering an effective modification strategy to improve their durability. Future research should further evaluate the long-term durability of CF-based densifiers under diverse environmental conditions, optimize dosage and processing parameters, and expand their practical application to broader engineering scenarios. These efforts will provide robust support for enhancing the durability and sustainability of concrete structures.

5 Outlook

To move beyond the short-term laboratory evidence presented here and secure CF-S2 as a dependable solution for aggressive service environments, further work must deepen both mechanistic understanding and field validation. Accordingly, future research will centre on four complementary directions:

1. Coupled high-humidity sulfate–chloride exposure–Verify CF-S2 performance under simultaneous SO_4^{2-} and Cl^- attack in saturated conditions.
2. Extended service testing–Prolong wet–dry cycling beyond 180 cycles and use mixed sulfate–chloride solutions to quantify long-term effects on chloride transport and reinforcement corrosion protection.
3. Service-life modelling–Calibrate multi-ion coupled transport–reaction models with the expanded dataset to generate quantitative service-life prediction charts that support mix design and durability specifications.
4. Mechanistic verification of the proprietary formulation–Because the complete recipe is confidential, FTIR, XPS and TGA will be employed to identify *in-situ* reaction products and substantiate the proposed pore-refinement mechanism.

Data availability statement

The original contributions presented in the study are included in the article/supplementary material, further inquiries can be directed to the corresponding author.

Author contributions

JL: Writing – review and editing, Formal Analysis, Data curation. PH: Methodology, Writing – review and editing, Investigation, Formal Analysis. HG: Investigation, Writing – review and editing, Formal Analysis. XW: Validation, Methodology, Writing – original draft. ZL: Validation, Writing – review and editing, Methodology, Data curation, Conceptualization, Investigation.

Funding

The author(s) declare that no financial support was received for the research and/or publication of this article.

Conflict of interest

Authors JL, PH, and HG were employed by Shanghai Transportation Construction General Contracting Co., Ltd.

The remaining authors declare that the research was conducted in the absence of any commercial or financial relationships that could be construed as a potential conflict of interest.

Generative AI statement

The author(s) declare that no Generative AI was used in the creation of this manuscript.

Publisher's note

References

Akpinar, P., and Casanova, I. (2010). A combined study of expansive and tensile strength evolution of mortars under sulfate attack: implications on durability assessment. *Mater. Constr.* 60, 59–68. doi:10.3989/mc.2010.47908

Andrade Neto, J. D. S., De La Torre, A. G., and Kirchheim, A. P. (2021). Effects of sulfates on the hydration of Portland cement – a review. *Constr. Build. Mater.* 279, 122428. doi:10.1016/j.conbuildmat.2021.122428

Aye, T., and Oguchi, C. T. (2011). Resistance of plain and blended cement mortars exposed to severe sulfate attacks. *Constr. Build. Mater.* 25, 2988–2996. doi:10.1016/j.conbuildmat.2010.11.106

Bary, B., Leterrier, N., Deville, E., and Le Bescop, P. (2014). Coupled chemo-transport-mechanical modelling and numerical simulation of external sulfate attack in mortar. *Cem. Concr. Compos.* 49, 70–83. doi:10.1016/j.cemconcomp.2013.12.010

Bassuoni, M. T., and Rahman, M. M. (2016). Response of concrete to accelerated physical salt attack exposure. *Cem. Concr. Res.* 79, 395–408. doi:10.1016/j.cemconres.2015.02.006

Campos, A., López, C. M., Blanco, A., and Aguado, A. (2018). Effects of an internal sulfate attack and an alkali-aggregate reaction in a concrete dam. *Constr. Build. Mater.* 166, 668–683. doi:10.1016/j.conbuildmat.2018.01.180

Chen, W., Li, K., Wu, M., Liu, D., Wang, P., and Liang, Y. (2023). Influence of pore structure characteristics on the gas permeability of concrete. *J. Build. Eng.* 79, 107852. doi:10.1016/j.jobe.2023.107852

Cheng, X., Tian, W., Gao, J., and Gao, Y. (2022). Performance evaluation and lifetime prediction of steel slag coarse aggregate concrete under sulfate attack. *Constr. Build. Mater.* 344, 128203. doi:10.1016/j.conbuildmat.2022.128203

Dhandapani, Y., and Santhanam, M. (2020). Investigation on the microstructure-related characteristics to elucidate performance of composite cement with limestone-calcined clay combination. *Cem. Concr. Res.* 129, 105959. doi:10.1016/j.cemconres.2019.105959

Fang, Z., Li, Z., Zhou, Y., Xie, Q., Peng, H., Zhou, S., et al. (2023). Effect of stray current and sulfate attack on cementitious materials in soil. *Constr. Build. Mater.* 408, 133723. doi:10.1016/j.conbuildmat.2023.133723

Fang, Z., Wang, C., Hu, H., Zhou, S., and Luo, Y. (2022). Effect of electrical field on the stability of hydration products of cement paste in different liquid media. *Constr. Build. Mater.* 359, 129489. doi:10.1016/j.conbuildmat.2022.129489

GB/T 176,Methods for chemical analysis of cement (2008).

GB/T 17671,Test method of cement mortar strength (ISO method) (2021).

GB/T 50081,Standard for test methods of concrete physical and mechanical properties (2019).

GB/T 50082,Standard for test methods of long-term performance and durability of ordinary concrete (2009).

Guo, Y., Wu, S., Lyu, Z., Shen, A., Yin, L., and Xue, C. (2021). Pore structure characteristics and performance of construction waste composite powder-modified concrete. *Constr. Build. Mater.* 269, 121262. doi:10.1016/j.conbuildmat.2020.121262

He, R., and Lu, N. (2024). Air void system and freezing-thawing resistance of concrete composite with the incorporation of thermo-expansive polymeric microspheres. *Constr. Build. Mater.* 419, 135535. (Luna). doi:10.1016/j.conbuildmat.2024.135535

He, R., and Lu, N. L. (2023). Unveiling the dielectric property change of concrete during hardening process by ground penetrating radar with the antenna frequency of 1.6 GHz and 2.6 GHz. *Cem. Concr. Compos.* 144, 105279. doi:10.1016/j.cemconcomp.2023.105279

He, R., Nantung, T., Olek, J., and Lu, N. (2023). Field study of the dielectric constant of concrete: a parameter less sensitive to environmental variations than electrical resistivity. *J. Build. Eng.* 74, 106938. doi:10.1016/j.jobe.2023.106938

Ikumi, T., Cavalaro, S. H. P., Segura, I., De La Fuente, A., and Aguado, A. (2016). Simplified methodology to evaluate the external sulfate attack in concrete structures. *Mater. and Des.* 89, 1147–1160. doi:10.1016/j.matdes.2015.10.084

Irassar, E. F. (2009). Sulfate attack on cementitious materials containing limestone filler — a review. *Cem. Concr. Res.* 39, 241–254. doi:10.1016/j.cemconres.2008.11.007

Kou, S.-C., and Poon, C.-S. (2013). Long-term mechanical and durability properties of recycled aggregate concrete prepared with the incorporation of fly ash. *Cem. Concr. Compos.* 37, 12–19. doi:10.1016/j.cemconcomp.2012.12.011

Kumar, R., and Bhattacharjee, B. (2003). Porosity, pore size distribution and *in situ* strength of concrete. *Cem. Concr. Res.* 33, 155–164. doi:10.1016/S0008-8846(02)00942-0

Kumar Mehta, P., and Monteiro, P. J. M. (1986). *Concrete: structure, properties, and materials*. Englewood, America: Prentice Hall.

Li, C., Jiang, L., Xu, N., and Jiang, S. (2018). Pore structure and permeability of concrete with high volume of limestone powder addition. *Powder Technol.* 338, 416–424. doi:10.1016/j.powtec.2018.07.054

Liu, K., Sun, Y., Shen, S., Sun, D., Wang, A., and Wang, Y. (2024). Application of sulfate ion fixation in internal sulfate attack: the gel containing barium salt. *Case Stud. Constr. Mater.* 20, e02873. doi:10.1016/j.cscm.2024.e02873

Mohan, M. K., Rahul, A. V., Van Stappen, J. F., Cnudde, V., De Schutter, G., and Van Tittelboom, K. (2023). Assessment of pore structure characteristics and tortuosity of 3D printed concrete using mercury intrusion porosimetry and X-ray tomography. *Cem. Concr. Compos.* 140, 105104. doi:10.1016/j.cemconcomp.2023.105104

Neville, A. (2004). The confused world of sulfate attack on concrete. *Cem. Concr. Res.* 34, 1275–1296. doi:10.1016/j.cemconres.2004.04.004

Nosouhian, F., Fincan, M., Shanahan, N., Stetsko, Y. P., Riding, K. A., and Zayed, A. (2019). Effects of slag characteristics on sulfate durability of Portland cement-slag blended systems. *Constr. Build. Mater.* 229, 116882. doi:10.1016/j.conbuildmat.2019.116882

Ohno, M., and Maekawa, K. (2025). Fully coupled physicochemical-mechanical modeling of sulfate attack-induced expansion in cement-based materials. *Cem. Concr. Compos.* 161, 106076. doi:10.1016/j.cemconcomp.2025.106076

Pang, Y., Wang, H., Tang, Q., Yang, L., and Wang, Q. (2024). Enhancing cement mortar hydrophobicity against dry-wet cycling sulfate attack using stearic acid modified mica powder via high-temperature stirring. *Constr. Build. Mater.* 441, 137556. doi:10.1016/j.conbuildmat.2024.137556

Qi, B., Gao, J., Chen, F., and Shen, D. (2017). Evaluation of the damage process of recycled aggregate concrete under sulfate attack and wetting-drying cycles. *Constr. Build. Mater.* 138, 254–262. doi:10.1016/j.conbuildmat.2017.02.022

Qin, S., Zou, D., Liu, T., and Jivkov, A. (2020). A chemo-transport-damage model for concrete under external sulfate attack. *Cem. Concr. Res.* 132, 106048. doi:10.1016/j.cemconres.2020.106048

Quan, X., Wang, S., Liu, K., Zhao, N., Xu, J., Xu, F., et al. (2021). The corrosion resistance of engineered cementitious composite (ECC) containing high-volume fly ash and low-volume bentonite against the combined action of sulfate attack and dry-wet cycles. *Constr. Build. Mater.* 303, 124599. doi:10.1016/j.conbuildmat.2021.124599

Salmas, C. E., and Androutsopoulos, G. P. (2001). A novel pore structure tortuosity concept based on nitrogen sorption hysteresis Data. *Ind. Eng. Chem. Res.* 40, 721–730. doi:10.1021/ie000626y

Singh, R. P., Vanapalli, K. R., Jadda, K., and Mohanty, B. (2024). Durability assessment of fly ash, GGBS, and silica fume based geopolymer concrete with recycled aggregates against acid and sulfate attack. *J. Build. Eng.* 82, 108354. doi:10.1016/j.jobe.2023.108354

Sun, C., Chen, J., Zhu, J., Zhang, M., and Ye, J. (2013). A new diffusion model of sulfate ions in concrete. *Constr. Build. Mater.* 39, 39–45. doi:10.1016/j.conbuildmat.2012.05.022

Sun, D., Wu, K., Shi, H., Zhang, L., and Zhang, L. (2018). Effect of interfacial transition zone on the transport of sulfate ions in concrete. *Constr. Build. Mater.* 192, 28–37. doi:10.1016/j.conbuildmat.2018.10.140

Tan, Y., Yu, H., Yang, D., and Feng, T. (2022). Basic magnesium sulfate cement: autogenous shrinkage evolution and mechanism under various chemical admixtures. *Cem. Concr. Compos.* 128, 104412. doi:10.1016/j.cemconcomp.2022.104412

Wang, H., Li, Y., Liao, H., Zou, D., and Liu, T. (2025). Deterioration mechanism of OPC mortar under combined chemical and physical sulfate attack in partial immersion. *Constr. Build. Mater.* 475, 141187. doi:10.1016/j.conbuildmat.2025.141187

Wang, K., Guo, J., Wu, H., and Yang, L. (2020). Influence of dry-wet ratio on properties and microstructure of concrete under sulfate attack. *Constr. Build. Mater.* 263, 120635. doi:10.1016/j.conbuildmat.2020.120635

Wei, Y., Chai, J., Qin, Y., Li, Y., Xu, Z., Li, Y., et al. (2021). Effect of fly ash on mechanical properties and microstructure of cellulose fiber-reinforced concrete under sulfate dry–wet cycle attack. *Constr. Build. Mater.* 302, 124207. doi:10.1016/j.conbuildmat.2021.124207

Xiangpeng, F., Liping, G., Runsong, B., Bangcheng, L., and Jiandong, W. (2023). Research progress on sulfate durability of high ductility cementitious composites. *Constr. Build. Mater.* 385, 131509. doi:10.1016/j.conbuildmat.2023.131509

Yu, Y., and Zhang, Y. X. (2018). Numerical modelling of mechanical deterioration of cement mortar under external sulfate attack. *Constr. Build. Mater.* 158, 490–502. doi:10.1016/j.conbuildmat.2017.10.048

Zhang, J., Shi, C., Zhang, Z., and Ou, Z. (2017). Durability of alkali-activated materials in aggressive environments: a review on recent studies. *Constr. Build. Mater.* 152, 598–613. doi:10.1016/j.conbuildmat.2017.07.027

Zhang, S., Tan, G., Qi, Z., Tian, B., Cao, J., and Chen, B. (2024). Relationship between the carbonation depth and microstructure of concrete under freeze–thaw conditions. *Materials* 17, 6191. doi:10.3390/ma17246191

Zhang, Z., Zhou, J., Yang, J., Zou, Y., and Wang, Z. (2020). Understanding of the deterioration characteristic of concrete exposed to external sulfate attack: insight into mesoscopic pore structures. *Constr. Build. Mater.* 260, 119932. doi:10.1016/j.conbuildmat.2020.119932

Zhao, L., Feng, P., Shen, X., Rong, H., Miao, C., and Geng, G. (2024). Mitigating chloride attack in cementitious materials without compromising other properties via the use of viscosity modifying admixture. *Cem. Concr. Compos.* 147, 105441. doi:10.1016/j.cemconcomp.2024.105441

Zheng, Y., Fan, C., Ma, J., and Wang, S. (2023). Review of research on Bond–Slip of reinforced concrete structures. *Constr. Build. Mater.* 385, 131437. doi:10.1016/j.conbuildmat.2023.131437